"Physics of Auroral Phenomena", Proc. XXIII Annual Seminar, Apatity, pp.33-37, 2000

Polar Geophysical Institute

ION DISPERSION FEATURES OBSERVED IN THE CUSP/CLEFT

M.Yu.Goncharova *(Polar Geophysical Institute, Apatity 184200, Russia)*

Abstract. The dynamic ion dispersion signature in the DMSP format, produced by a plane particle injection source displacing with no inertia across the magnetic field lines at a fixed field-aligned distance is calculated in presence of the ionosphere convection flow. Easy to see that in absence of the source displacement the convection-produced dispersion signature has its lower energy cutoff with the precipitation onsets at each discrete energy level matching the velocity filter effect formula with no deviations, e.g., smoothly. In contrast to this the horizontal displacement of the precipitation source added produces regular shifts of the convection-formed dispersion signature in the direction of the source motion, resulting into the stairlike lower energy cutoff. Stairs are observed in the most of ion dispersion signatures at DMSP/F7. In the model the lower energy cutoff distortions occur on account of violation of the arrival sequence for particles with different energies coming to the same precipitation site. The model predicts for the velocity fitting of the general ion dispersion signature cutoff to be nearly the source & convection velocities vector difference.

Introduction

In satellite observations of precipitations the discrepancy between the observed and velocity filter effect-predicted distributions of the field-aligned energies versus latitude are very common [Lockwood *et al.,* 1993] since the predictions are ultimately based on a fixed injection source assumption. The stairlike lower energy cutoff is one amongst the unpredicted features. The large-scale stairs often cover several steps both in time and energy resolution. Therefore the cutoff doesn't match perfectly the fit derived from the fixed precipitation source model. The stair edge faced to the energy axis allows the fit with another velocity, e.g., more than one distinctive velocity values are observed at the same place, related to the common lower energy cutoff and to its element. It means these velocities characterize different processes. The dispersion signature modeling examples can be found in [Onsager *et al*., 1993; Lockwood *et al.*, 1998]. In spite of a wide assortment of contributing factors taken into account when reconstructing the evolution of the observed signature in the inverted time followed by theoretical reconstruction the unexplained characteristics of the typical dispersion shape still remain. The possible problem for calculations was the temporal superposition of the particle injection/detection processes. After separating the two processes the convection-independent horizontal shift of the injection source can be taken into account, what produces, as a function of sort of motion, not the characteristic stairlike shape of the lower energy cutoff only, but its spatial curvature variations as well, including sudden changes of the particle energy declines and injections superimposed in latitude. As an intermediate part of another investigation, this modeling was finalized in August 1998, e.g., before Lockwood *et al.* [1998] have published their results with sufficiently improved reconstructed dispersion signatures. The work have been postponed for finding the statistical evidence of the injection source motion effect to the dispersion-forming velocity - solar wind conditions dependence. These velocities, poleward-directed, were found to diminish in value towards larger steady B_z southward (Goncharova *et al.*, [1999]) while their latitudes of observation/source projection were lowering. This unexpected velocity behavior is difficult to relate to the high-latitude dayside convection for it must strengthen in this case. A stationary dependence of the velocity meridian component on the injection source latitude was obtained as well.

The main indicators of the classic ion dispersion signature (see Newell and Meng, [1995], plate 1 for example) seen in DMSP F7 spectra are as follows:

1) smooth lower energy cutoff which can be satisfactorily fitted by the velocity filter effect formula for the fixed injection source position:

$$v_{tff} = \frac{(s_l - s_h)}{h\sqrt{m/2}} \cdot \frac{\sqrt{E_h E_l}}{(\sqrt{E_h} - \sqrt{E_l})} \tag{1}$$

where v_{eff},- is an effective (obtained from cutoff fit) velocity of the horizontal shift of particles, h - their field-aligned height of injection, m - the proton mass, E_h и E_l - the field-aligned harder and softer proton energies respectively, s_h и s_l - latitudinal distance between the source projection and precipitation site;

2) intersection with the horizontal axis of the dispersion signature itself or of the fitting curve satisfactorily matching its lower energy cutoff; (see also Lockwood *et al*., [1993]);

3) narrowing of the dispersion signature vertical width (along energy axis) towards lower energies (see color plates in Lockwood *et al.*, [1993]).

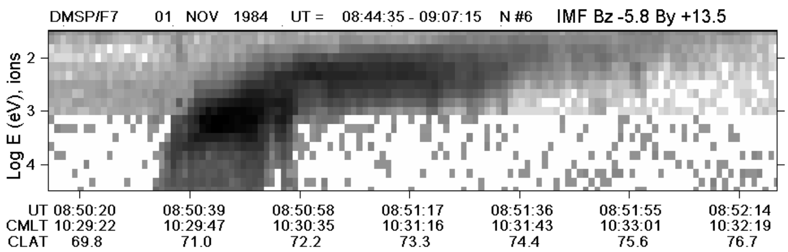

Fig.1. Dispersion signature produced by a slightly agile source of ticles.

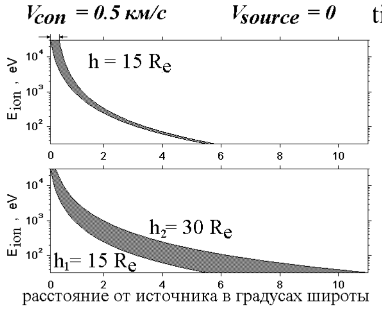

Fig. 2. Source geometry effect. Upper panel: the dispersion from a steady disc with horizontal size 0.3° in ionosphere projection. Lower panel: the dispersion from a steady vertical line open for particle access within 15 - 30 R_e

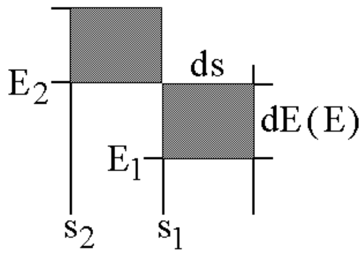

Fig. 3. A sketch representing the different energy detection in the DMSP/F7 format: 19 narrow energy channels of 0.1 E_i width are stepped in a way $E_{i+1} = E_i^{1.46}$. During the resolution time 1 s the satellite moves by ds~ 7.5 km in latitude.

The convection-shaped ion dispersion signature from a steady source

1.Source geometry effects.

In figure 2 the theoretical dispersion signature from the steady source in the ionosphere reference frame is shown. The source has a finite length in latitude (upper panel) or in field-aligned height (lower panel). The finite horizontal size of the source becomes noticeable if it exceeds ~50 km in ionosphere projection. The divergence between the lower and upper cutoff fits by (1) do the character of the dispersion produced by a thin vertical line.

In Fig.3 the sketch represents the particle detection at discrete energy levels in the DMSP/F7 format (see also Newell and Meng, [1995]). It indicates the key role in the observed energy versus latitude dependence belongs to the simultaneity (within the time resolution) of the different energy particle detection at the same height in a wide latitude range. The necessary conditions for the simultaneous particle occurrence in the two narrow energy ranges are easy to obtain:

a) $\tau_1=\Delta t+\tau_2$, where $\tau_i = h/v_{||i}$ - the time-of-flight of i^{th} energy level particle, Δt - the time difference between he injection moments;

b) T > $|\tau_1 - \tau_2|$, where T is the point source operating time, reflected in the “life time” of the filled cell in the spectrogram.

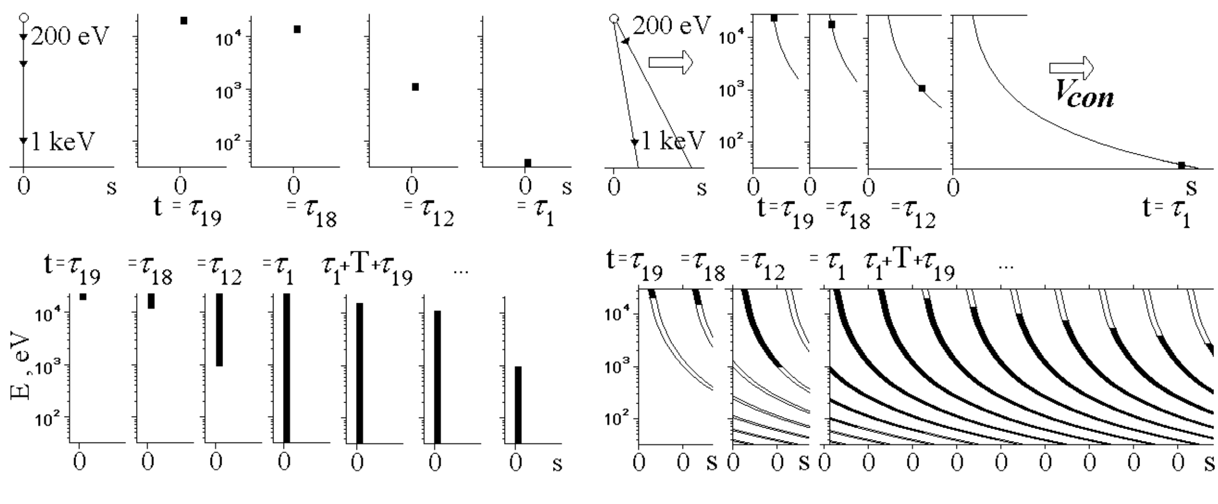

Fig. 4. Expected spectra for impulsive (upper) and continuous, lasting T s (lower panel), injections obtained for an almost point-like source with no (left) and yes (right panel) convection shift added, snapped in moments t corresponding to the times-of-flight τ_i for parallel energies registered in DMSP format. Zeros mark the source position for each spectrum.

2. Source operating manner effect.

In figure 4 the dynamic evolution of the dispersion from the steady source for a single pulse and continuous operating manner are shown. The observer in the ionosphere would detect the dispersion from the single impulsive particle injection as a filled cell falling down along the energy axis, whereas the dispersion from the source operating continuously during some time T will be regarded as a falling vertical line. The horizontal shift added, the trajectories of falling filled cells get distorted in a manner (1) allowing to handle with a set of trajectories as with the real dispersion signatures. From Fig. 4, right lower panel, where 6 trajectories of falling cells for the 6 time moments selected are hold on with spatial shift, it particularly follows that injections from several non-synchronously operating sources, ranged in latitude, may be overlapped both in energy and latitude in the final spectrum, similarly to the overlapping injections reported in Norberg., *et al* [1994]. If the switching on/off moments for the two neighboring sources coincide, their operating manner can be simulated with a single source displacement. In this case, as the model predicts, the possibility for overlapping injections remains.

3. Temporal evolution of the dynamic spectra shaped with convection and source motion for continuous injections.

7

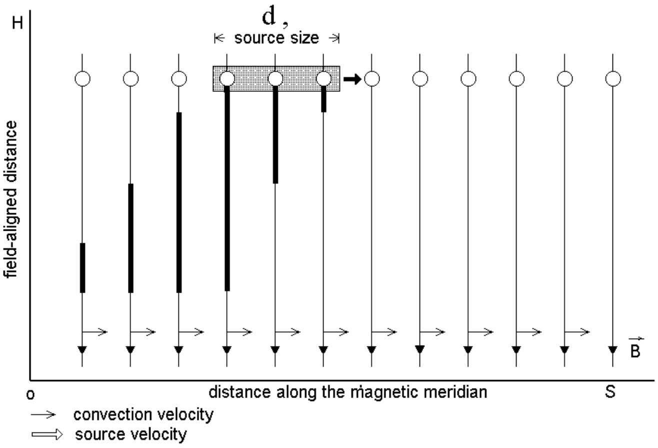

Fig. 5. The model of the plane injection source, size-limited, moving across the magnetic field lines with no inertia.

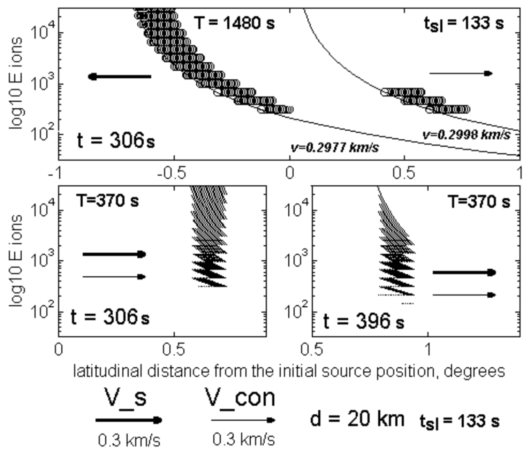

Fig. 6. Distinctions in the convection and source motion-shaped dispersion signatures.

Source is assumed to be plane (Fig. 5), of ~20 km width in latitude at ionosphere level, (~V_{con}/V_{SW} times less than the outer cusp size, ~3 R_E) situated at field-aligned distance of ~10 R_E. The operating time at any fixed point turns into the 'particle flux lifetime' t_{sl} at the spectrogram cell. For moving source t_{sl} is set to be the source width divided by its velocity in the ionosphere reference frame, thus the total source operating time T> t_{sl}.

The source fixed, the convection shapes the parallel energy versus latitude functional dependence, due to distinctive times of flight τ_i, defining the simultaneity of observation as well as t_{sl}. In this case the lower energy cutoff will be looked as a sequence of points approximated in Fig. 6 (upper panel) with a velocity of 0.2998 km/s (thin curve) versus the given convection velocity of 0.300 km/s. The stairs observed between neighboring energy levels match fit (1) with no deviations since they reflect the energy measurement discreteness and are of equipment origin. In contrast to it, the source motion added, the precipitation site sequence may be violated. The fitting velocity value becomes sensitive to the probe point choice (-0.2977 km/s versus the given source velocity of -0.300 km/s for the same E_{high}, E_{low} as in the convection case in Fig. 6, right upper panel) what gives an evidence the distortions occur in the lower energy cutoff. The program allowed to identify points in spectrogram corresponding to the same injection points of Fig. 5 by means of relating lines, which (Fig. 6) reflects, consequently, the convection velocity, since the non-inertial motion of the source does not contribute the particle impulse. In Fig. 6, lower panel, the dispersion signature from the source attached to the drifting magnetic flux tube is simulated this way; with the higher energies vanishing if from some moment the source activity interrupts.

In Fig. 7, left upper panel, the lower energy cutoff is shaped by the source latitudinal displacement with -0.15 km/s velocity value together with the convection flow (0.3 km/s). The cutoff can be fitted with a velocity value +0.4471 km/s ≈ | $\boldsymbol{v}_{con}$ - $\boldsymbol{v}_s$|. The reason for inaccuracy is the same violation of the particle precipitation site sequence by the source motion. In Fig. 7, middle panel, two spectral snapshots are superimposed, previous (empty circles) onto the next one (filled circles), demonstrating that by this reason the dispersion signature moves behind the source discretely in energy. Thus, the equipment origin stairs get distorted by source motion, marking the cutoff intervals shaped with the convection and source velocity vector difference $\boldsymbol{v}_{con}$ - $\boldsymbol{v}_s$. When the |$\boldsymbol{v}_{con}$|>| $\boldsymbol{v}_{con}$ - $\boldsymbol{v}_s$| condition is satisfied, the large-scale stair occurs on the lower energy cutoff at some moment (see Fig. 7, left lower panel, left image). Otherwise, the momentary cutoff is shaped with the velocity vector difference alone.

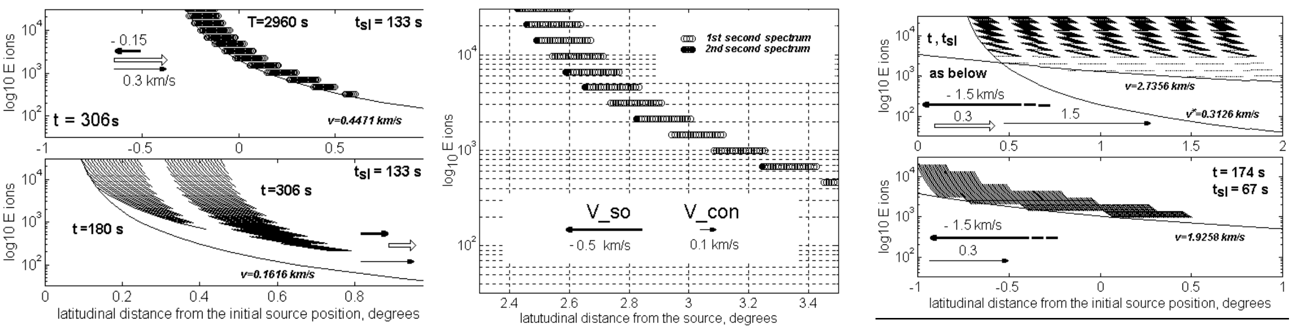

Fig. 7. The cutoff distortions seen in the momentary spectra (left and middle panels) and spectrogram (right panel).

Jumping source or multiple sources operating simultaneously also would produce the stair-like lower energy cutoff. The shift of their launch points, also non-inertial one, produces a set of dispersion signatures with a common cutoff reflecting the launch point velocity $\boldsymbol{v}_0$ and convection velocity $\boldsymbol{v}_{con}$ (Fig. 7, right panel). Insofar, to measure the convection velocity at some interval of the lower energy cutoff specific source motion conditions are necessary.

In Fig. 8 the lower energy cutoff of the dispersion signature reveals 4 stairs resembling that one of Fig. 7. The general cutoff allows a fairly smooth common fit with $\boldsymbol{v}$~ -1.86 km/s, and the lower energy cutoff components faced to the energy axis are fitted with $\boldsymbol{v}$*~ 0.29 км/c value. Plane stair edges faced to the X-axis suggest that no continuous source drift have been added, and the cutoff energies increasing towards pole followed by the highest energies vanishing indicate the injection onset positions moved poleward with time in discrete manner while the source operating time diminished from ~435 s at -73° dawn to ~78 s at -78° CLAT.

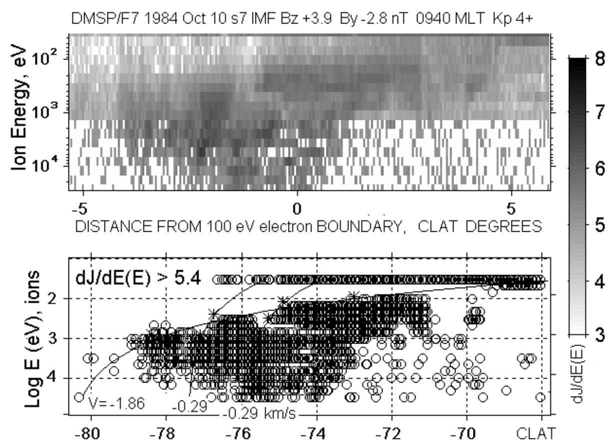

For 100 and 313 eV particles (Fig. 8) injected at a field-aligned distance of ~15 R_E assumed the times-of-flight are 691 and 391 s respectively, and the |-76.8°-(-73°)|=3.8° CLAT interval between their first occurrences gives v_0=+1.6 km/s at 800 km altitude. Note that the general cutoff-fitting velocity which can not be that of convection or source drift alone because of the large-scale stairs observed.

The velocity fitting the energy-faced stair edges may stand for, in turn, either the convection/source drift velocity or for their vector difference. The latter case is more probable since the zero meridian convection velocity within 4° in latitude is hardly expected. Substituting $\boldsymbol{v_{con}}$-$\boldsymbol{v_0}$ =-1.86 km/s, $\boldsymbol{v}^*$=$\boldsymbol{v_{con}}$-$\boldsymbol{v_s}$=-0.29 km/s, and v_0=+1.6 km/s one obtains -0.26 km/s for the convection velocity; for the source drift velocity +0.03 km/s rests

The solar wind velocity was V_{SW}~725 km/s and the steady IMF B_z=+3.9 nT for the observation time. Assuming the down-to-dusk magnetosphere width in the X=3÷0 R_E (GSM) plane to be of ~20÷30 R_E and the polar cap boundary position at ~-74° CLAT one obtains ~3÷6.5 km/s for the predicted convection velocity in pre-noon sector, >> 0.29 km/s. (Note the least estimate is close to the calculated injection onset site velocity and may reflect the relation of the source position to the solar wind magnetic field progressing tailward. However, in the considered figure *no smooth nor any fit with similar velocity value is possible).*

That is the dispersion contains information on the solar wind induced electric field not only, but on the injection source displacements as well. The smallness of the observed velocity $\boldsymbol{v}^*$ and calculated convection velocity v_{con} in Fig. 8 would mean the geomagnetic activity (Kp=4+) effecting the dayside convection.

Summary

1. Simple theoretical model of the dispersion signature forming contributed by the convection and precipitation source horizontal displacement is proposed. It is shown that:

2. The source geometry effects the dispersion signature width in energy and changes its overall shape.

3. The lower energy cutoff formed by the convection velocity filter effect distinguishes from that one formed by the source velocity filter effect by smoothness in contrast to distortions occurring due to violation of the particle precipitation site sequence. As a result, the fitting velocity is not accurately equal to the real dispersion-forming velocity.

4. The convection and source motion operating together, the cutoff is shaped by the vector difference of their velocities and by the convection velocity, $v=v_{con}-v_s$. Continuos horizontal drift of the source leads to the lower energy cutoff fitting velocity change and reveals itself via small-scale cutoff latitudinal deviations from its fit. The cutoff distortions related to the effective factor change (Fig. 7, left) have the edge faced to the energy axis been defined by the minimum, and the other edge by the maximum of the two values. The multiple elements of this kind would mean the several sources operating together while their occurrence site displaces with time discretely at a certain velocity which also contributes the cutoff fit. For this case the formula $v=v_{con}-v_s$ is valid too.

The stair-like lower energy cutoffs with micro-deviations from fit (1) are typical for the ion dispersions observed onboard the DMSP satellites (see, for example, Newell and Meng, [1995]), as well as with large-scale stairs giving an evidence for the source motion contribution into the cutoff forming. Thus most of the velocities obtained from the lower cutoff fit correspond to the convection and source velocity vector difference.

Acknowledgments. The author acknowledges Drs. D.G.Sibeck and P.N.Newell for kind permission to use AMPTE IRM and DMSP/F7 data, Dr. V. N. Kriviliov for the computer data processing, and Dr. Yu. P. Maltsev for attention to work and discussion.

References

Goncharova, M. Yu., W. Lyatsky, V. Kriviliov and D. G. Sibeck, Ion energy dispersion events in the cusp/cleft and mantle: general dispersion signature, *Proceedings of the 22nd Annual seminar*, *Apatity, 23-26 March 1999, PGI-99-01-107*, 33, 1999

Lockwood, M., W. F. Denig, A. D. Farmer, V. N. Davda, S. V. H. Cowly and H. Luhr, Ionospheric signatures of pulsed reconnection at the Earth's magnetopause, *Nature*, 361, 424-427, 1993.

Lockwood, M. C. J. Davis, T. G. Onsager, J. D. Scudder, Modeling signatures of pulsed magnetosphere reconnection in cusp ion dispersion signatures seen at middle altitudes, *Geophys. Res. Lett., 25,* 951-954, 1998.

Newell, P.T., and Meng Ch.-I., Cusp low-energy ion cutoffs: A survey and implications for merging, *J. of Geophys. Res., 100,* 21,943-21,951 , 1995

Norberg, O., M. Yamauchi, L. Eliasson, and R. Lundin, Freja observation of multiple injection events in cusp, *Geophys. Res. Lett., 21*, 1919-1922, 1994

Onsager, T.G., C.A. Kletzing, J. B. Austin, and H.MacKiernan, Model of Magnetosheath plasma in the magnetosphere: cusp and mantle particles at low altitudes, *J. of Geophys. Res., 20*, 479-482, 1993